Charge transport by ion translocating membrane proteins on solid supported membranes

Karsten Seifert, Klaus Fendler, and Ernst Bamberg
Max-Planck-Institut für Biophysik, D-6000 Frankfurt 70, Germany

ABSTRACT A new method for the investigation of ion translocating membrane proteins is presented. Protein containing membrane fragments or vesicles are adsorbed to a solid supported membrane. The solid supported membrane consists of a lipid monolayer on a gold evaporated or gold sputtered glass substrate which is coated with a long chained mercaptan ($CH_3(CH_2)_mSH$, $m = 15, 17$). Specific conductance and specific capacitance of the solid supported membrane are comparable to those of a black lipid membrane. However, the solid supported membrane has the advantage of a much higher mechanical stability. The electrical activity of bacteriorhodopsin, Na,K-ATPase, H,K-ATPase, and Ca-ATPase on the solid supported membrane is measured and compared to signals obtained on a conventionally prepared black lipid membrane. It is shown that both methods yield similar results. The solid supported membrane therefore represents an alternative method for the investigation of electrical properties of ion translocating transmembrane proteins.

INTRODUCTION

Adsorption of membrane fragments or vesicles containing ion translocating membrane proteins to a black lipid membrane (BLM) has been used to study time resolved charge translocations of these enzymes (e.g., Bacteriorhodopsin (4, 8), Na,K-ATPase (11), Ca-ATPase (14)). Low specific conductance and high specific capacitance of the BLM leads to transient capacitive currents after activation of the ion pumps. Analysis of these currents has provided information about charge transport during distinct partial reactions of a variety of membrane proteins (4, 5, 8, 11, 12, 14, 18, 27).

The advantages of the BLM are its low specific conductance and its high specific capacitance. Low conductance is important because of the high background noise associated with a high conductance sample. High specific capacitance yields a large signal in current measurements (4). The major drawbacks are mechanical instability and small surfaces (≈ 0.01 cm^2).

As shown recently by Florin and Gaub (13), the solid supported membrane (SSM) maintains high specific capacitance and low specific conductance but at the same time has a large surface (≈ 0.25 cm^2) and mechanical stability as compared to the BLM. Using this device, charge transport in ion pumps can be studied in an environment comparable to that of a BLM.

MATERIALS AND METHODS

Chemicals

Diphytanoyl phosphatidylcholine (PC; synthetic; Avanti Polar Lipids, Inc., Pelham, AL), phosphatidylserine (PS; bovine brain; Avanti Polar Lipids, Inc.), and octadecyl amine (purity 98%; Riedel-DeHaën AG, Seelze-Hannover, Germany) were used.

Monolayers were prepared from PC and octadecyl amine (60:1, wt/wt) or PC and PS (4:1, vol/vol, PC/PS) both 1.5% in *n*-decane. The lipid solutions were prepared as described in Bamberg et al, 1979 (4). All other chemicals were purchased in analytical grade.

Caged ATP, a photolabile, inactive analogue of ATP used for the experiments with different ATPases, was prepared by a method described by Fendler et al., 1985 (11) and kindly provided by E. Grell (MPI für Biophysik, Frankfurt/M., Germany).

Purple membrane (PM) fragments containing bacteriorhodopsin (BR) were prepared according to Stoeckenius and Kunau, 1968 (35) and Oesterhelt and Stoeckenius, 1974 (28). The PM suspension had a optical density of $OD_{568\,nm} = 1.6$ (protein concentration 656 $\mu g \cdot ml^{-1}$). A typical PM fragment has a diameter of about 0.5 μm and a thickness of ~4.8 nm (17, 36).

Membrane fragments containing Na,K-ATPase (protein concentration 2–3 $mg \cdot ml^{-1}$, ATPase activity 20 $\mu mol\ P_i \cdot mg^{-1}protein \cdot min^{-1}$) from pig kidney were prepared as described by Jørgensen, 1974 (20, 21). H,K-ATPase containing vesicles (protein concentration 10 $mg \cdot ml^{-1}$, ATPase activity 1.7 $\mu mol\ P_i \cdot mg^{-1}protein \cdot min^{-1}$) from pig stomach were prepared as described by Ljungström et al., 1984 (25) and Saccomani et al., 1977 (32). Vesicles containing Ca-ATPase (protein concentration 11 $mg \cdot ml^{-1}$, ATPase activity 0.8 $\mu mol\ P_i \cdot mg^{-1}protein \cdot min^{-1}$) from sarcoplasmic reticulum from rabbit skeletal muscle were prepared according to Hasselbach and Makinose, 1963 (15).

The ATPase containing membrane fragments and vesicles have typical diameters of ~100–300 nm (16, 33). The thickness of the fragments is ~4 nm.

Gold electrodes

Glass plates (7×25 mm^2) were cleaned, dried, brought into an atmosphere of dichlorodimethyl silane for ~60 s, and then stored for 60 min at 130°C to allow the silane to react with the glass surface. The silanized glass plates were then sputtered with a gold layer. Sputtering was performed under an argon atmosphere of $50–70 \cdot 10^{-3}$ torr, with a sputter current of $35–45 \cdot 10^{-3}$ A and a sputter yield of 0.2–0.4 nm/s without cooling the substrate. The final thickness of the gold layer was 50 to 100 nm. The silanization procedure makes the glass surface hydrophobic and enhances the stability of the gold layer in the electrolyte. We used masks to obtain well defined gold covered areas on the glass support: a circular disk with a thin connecting line (Fig. 1 *A*).

The freshly deposited gold films were incubated in a mercaptan solution for 6 h at 30°C. We used a solution of 1 mM hexadecyl mercaptan (C_{16}-mercaptan; Fluka, Neu-Ulm, Germany) or octadecyl mercaptan (C_{18}-mercaptan; Aldrich, Steinheim, Germany) in ethanol. After mercaptan incubation, the surfaces were rinsed with ethanol and then dried. At this stage the electrodes can be stored dust-free for several days without significant loss of quality.

Correspondence should be directed to Karsten Seifert, Max-Planck-Institut für Biophysik, Kennedyallee 70, D-6000 Frankfurt 70, Germany.

0006-3495/93/02/384/08 $2.00

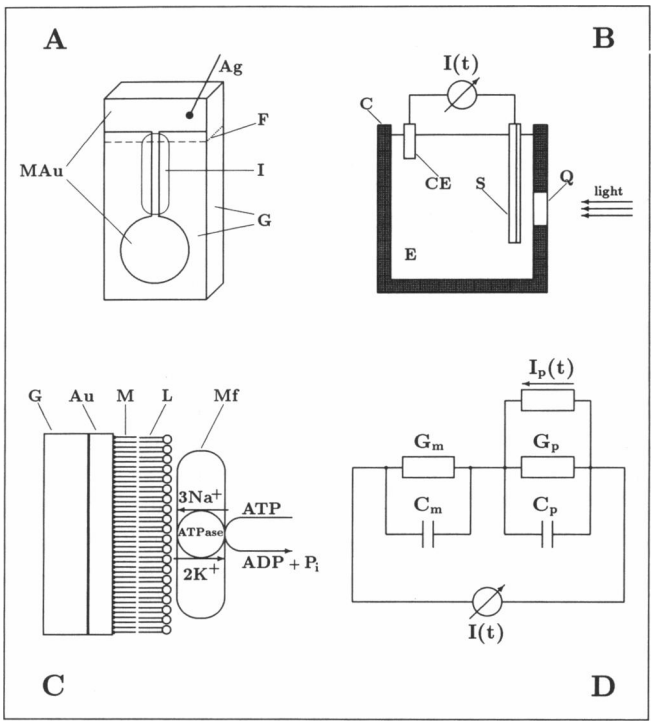

FIGURE 1 Experimental setup. (*A*) Macroscopical structure of a mercaptan treated gold electrode. Ag: connecting silver wire; F: filling level; G: glass support; I: insulating coating; MAu: mercaptan treated gold surface. (*B*) General experimental setup. C: cuvette; CE: counter electrode; E: membrane fragments containing electrolyte solution; Q: quartz window; S: solid supported membrane. (*C*) Microscopical structure of the SSM in the case of adsorbed membrane fragments containing Na,K-ATPase. G: silanized glass; Au: gold layer; M: mercaptan monolayer; L: lipid monolayer; Mf: membrane fragment. (*D*) Electrical equivalent circuit. $I_p(t)$ is the time-dependent pump current generated by the proteins. $I(t)$ is the time-dependent current which is measured in the outer circuit. The SSM is characterized by the specific capacitances C_p, C_m and by the specific conductances G_p, G_m of the membrane fragments and the SSM, respectively.

The connecting line was covered with nail polish as an electrically insulating coating. The circular disk remains as the only accessible mercaptan treated gold surface.

Lipid coating and SSM

The gold surface of an area of $A = 0.25\ cm^2$ was coated with 10 μl of an appropriate lipid solution while the glass plate was held horizontally. During this procedure the electrode was exposed to air. The incubation time was between 2 and 3 min. Then the lipid coated gold electrode was brought into a electrolyte filled teflon cuvette as shown in Fig. 1 *B*. Vertical positioning of the gold electrode ensures the run off of excess lipid solution and the formation of the monolayer. The lipid coated gold electrode was connected to a low noise current amplifier (gain: 10^6–10^8 V/*A*) via Ag/AgCl- or platinized Pt-electrodes. The output signals of the current amplifier were filtered (risetime: 1 μs–1 ms), recorded with a digital storage oscilloscope, stored, and analyzed with a personal computer.

Cuvette setup and illumination

The teflon cuvette (Fig. 1 *B*) had a volume of ~2.0 ml. The temperature was kept at 21°C via thermostat (RCS; MGW-Lauda, Lauda/Königshofen, Germany). A quartz window enabled the passage of visible and UV light.

For experiments with BR using stationary illumination, a halogen (HGL 12 V 250 W; Philips, Eindhoven, The Netherlands) or a high pressure Hg-lamp (HBO 200 W/2; Osram, Germany) was used. The spectral bandpass was limited by a heat protection filter (KG3; Schott, Mainz, Germany) and a cut-off filter ($\lambda \geq 495$ nm; Schott). The irradiance at the surface of the SSM was 400 mW/cm^2 ($495 \leq \lambda \leq 700$ nm). Lower irradiances were obtained with neutral density filters (0.1–70% transmission; Schott).

For the study of the kinetics of BR, we used an excimer laser pumped dye-laser (FL 2001; Lambda Physik, Göttingen, Germany) with a wavelength of $\lambda = 575$ nm, a pulse duration of 10 ns, and an energy density of ~100 μJ/cm^2 at the surface of the SSM.

For concentration jump experiments with ATPases, we used an excimer laser (EMG 100; Lambda Physik) with a wavelength of $\lambda = 308$ nm, a pulse duration of 10 ns, and an energy density of about 20 mJ/cm^2 at the surface of the SSM.

The SSM was always positioned perpendicular to the optical axis (parallel to the cuvette window). Caged ATP adsorbs light in the UV range with an absorption maximum at ~260 nm. At the wavelength of the exciting laser light of 308 nm the specific absorbance was $\epsilon_{\text{caged ATP,308 nm}} = 2440\ M^{-1}cm^{-1}$ (7). To minimize this absorption before the light reached the SSM, the thickness of the fluid layer between the SSM and the window of the cuvette was kept <2 mm corresponding to an optical density of $<5 \cdot 10^{-2}$ (89% transmission) at 100 μM caged ATP.

RESULTS

Properties of the SSM

As described in Materials and Methods, a lipid coating was formed on a mercaptan treated gold surface on a glass support. This was achieved by the combination of two different methods of monolayer assembly on solid supports.

It has been shown that mercaptan monolayers assemble spontaneously on clean gold surfaces from solutions of alkyl mercaptans in ethanol. The mercaptan molecules are probably bound covalently to the surface and build densely packed two-dimensional crystalline structures with the alkyl-chains tilted to the surface normal by 30° (1, 2, 3, 24, 42).

Other investigations demonstrated the spontaneous formation of lipid monolayers on alkyllated planar glass surfaces (41). Long chained alkylsilanes were used to obtain hydrophobic glass surfaces and the lipid monolayer formation was explained by the interaction between the hydrophobic alkylchains of the silane and the lipid molecules.

For the electrical measurements described here, metal surfaces were required. Clean gold surfaces are hydrophilic (34). The gold surfaces were made hydrophobic by alkyllation with a long chained mercaptan in ethanol. In the same way as lipid monolayers assemble on alkyllated glass surfaces (41), we assume that a monolayer is formed on mercaptan coated gold surfaces by spontaneous self-assembly. Florin and Gaub justified this assumption at least for a substantial part of the lipid film (13).

C_{18}-mercaptan pretreated SSMs were observed to be more stable than C_{16}-mercaptan pretreated ones. So, in all experiments reported here, C_{18}-mercaptan pretreated SSMs were used.

To ensure the correct preparation of the electrodes and the development of the SSMs, their electrical conductance and electrical capacitance were recorded. The gold layer served as one electrode. As counter electrodes Ag/AgCl- or platinized Pt-electrodes were used.

In the absence of an external voltage, rest currents were observed indicating the existence of inherent potentials. These potentials were estimated to be −150 to −250 mV by suppression of the rest current with an external potential. The inherent potential dropped across both the mercaptan and the lipid layer but apparently did not damage them.

For a conventional BLM built up from PC and octadecyl amine, the specific electrical conductance and the specific electrical capacitance were estimated to be G_m = 5.0 nS/cm^2 and C_m = 500 nF/cm^2, respectively. These values were obtained by observing the stationary current following a voltage step and by observation of the rectangular current response to an applied triangular voltage respectively. As shown by Florin and Gaub (13), one obtains comparable conductances and capacitances with the SSM.

Direct voltage methods are only partially applicable in the case of a SSM because of the underlying totally polarizable gold electrode which leads to time dependent decreasing currents. So no definite value for the electrical conductance of the SSM can be given with this method. It was used, however, to compare different SSM preparations. Therefore, the relaxing electrical current 30 s after an applied voltage step (50 mV) was observed. For the best preparations of SSM, meaning high stability, this method led to conductances of 2–10 nS/cm^2. The application of triangular voltages (0.5 Hz, ΔU_{pp} = 30 mV) led to almost rectangular current responses. Capacitances of about 100 nF/cm^2 were estimated.

With the Mueller-Rudin BLM life-times of about three to six hours are typical. Especially after addition of protein containing membrane fragments, vesicles, ionophores or uncouplers the BLM may become unstable. Care must be taken to avoid mechanical perturbations, which may destroy the BLM.

A typical SSM was stable for at least 20 h. During this time, the electrical conductance was comparable to the conductance of a BLM and remained constant. We performed experiments with bacteriorhodopsin containing PM fragments lasting over 48 h without significant changes in the signal quality. For times larger than 20 h, the conductance increased by two or three orders of magnitude. If the inherent electrode potential was compensated, the SSM showed the same behavior as without compensation. Mechanical perturbations, which usually destroy a BLM, did not influence the life-time of a SSM.

Photoartefact

In the absence of protein or caged ATP, light induced signals were observed with the SSM. In the following, these signals are referred to as photoartefacts. Shape and magnitude of these artefacts were variable even under constant conditions. As expected, the artefacts were especially large for UV light. In the presence of caged ATP, the artefacts were larger than in its absence. In addition, the artefacts depended on the electrolyte composition and on the external voltage and were much larger compared with those obtained with the BLM. The artefacts distorted the protein generated electrical signals for times shorter than 5 ms if an excimer laser was used for excitation. In dye-laser experiments, the artefacts were smaller and only the first μs of the signal were distorted.

There might be at least four probable sources of artefacts: the photoeffect on the gold surface following the absorption of photons in the metal surface, charge separation in caged ATP molecules situated on the surface of the lipid layer, proton release from caged ATP during the photolytic cleavage (7), and charge separation in the lipid or mercaptan molecules after absorption of photons. Depending on the experimental conditions all of these effects may contribute more or less to the photoartefact and make it variable. The fact that the artefact is larger than in the case of the BLM, is probably due to the photoeffect after absorption of photons in the gold surface.

Electric signals generated by ion translocating proteins

After electrical characterization of the SSM, a suspension of protein containing membrane fragments or vesicles was added to the cuvette under stirring. In most cases, 30 min after addition of the suspension, the adsorption of fragments or vesicles to the SSM was completed. The termination of the adsorption process was indicated by the end of the increase of the light induced electrical signal.

For a BLM with sufficiently low conductance, transient currents can be observed when the adsorbed ion pumps are activated (4, 10, 23), i.e., the BLM is used as a capacitive electrode. If the conductance of the SSM is comparable to that of a BLM, similar electrical phenomena are expected.

Bacteriorhodopsin

BR is the light-driven proton pump found in the PM of the archaebacterium *Halobacterium halobium.* In the light-adapted form it contains all-trans retinal as a chromophore. After light excitation, BR passes through a photocycle, returns to its ground state via a series of intermediates, and thereby translocates protons through the PM (36).

50 μl of a sonicated (30 s) suspension of light-adapted PM ($OD_{568\,nm}$ = 1.6) in H_2O were added to the cuvette.

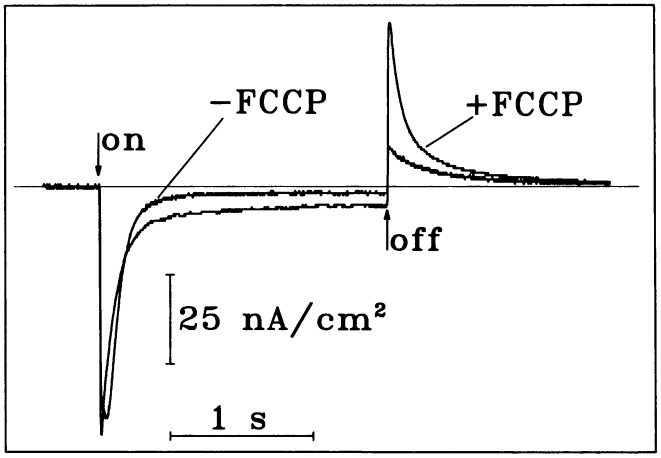

FIGURE 2 Bacteriorhodopsin. Light-induced transient current density in the presence of bacteriorhodopsin containing purple membranes under stationary illumination. The arrows indicate switching on and of the light. The traces are recorded in the absence (−FCCP) of and after addition (+FCCP) of 14 μM of the proton carrier FCCP. Conditions: SSM formed from PC + octadecyl amine; 100 mM NaCl, 10 mM Na-Citrate/HCl, pH = 6.03.

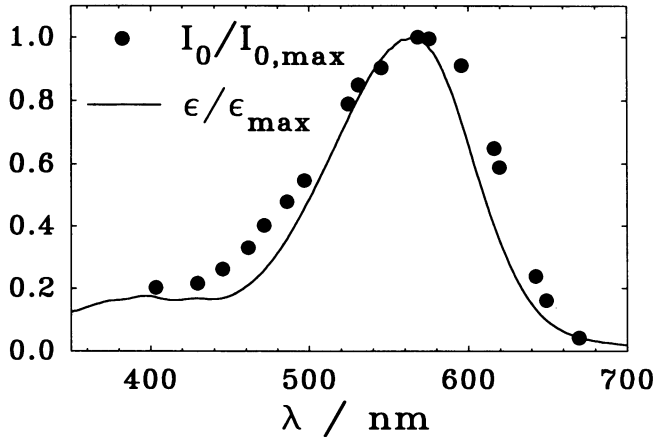

FIGURE 4 Bacteriorhodopsin. The action spectrum of BR (under stationary illumination) shows the normalized initial current density $I_0/I_{0,max}$ as a function of wavelength λ. The solid line represents the normalized absorption ϵ/ϵ_{max} of BR. Conditions as in Fig. 2.

Light induced transient electrical currents were observed as shown in Figs. 2 and 3. The direction of the current corresponds to the translocation of protons towards the SSM. The current density I rises to its peak value I_0 and then decays with a characteristic relaxation time τ to a stationary value which depends on the SSM conductivity. Peak current densities I_0 of ~60–200 nA/cm² were obtained. The specific conductance of the SSM obtained with the direct voltage method under these conditions was 1.7 nS/cm². The second trace (labelled "+FCCP") in Fig. 2 shows a signal from the same experiment 45 min after addition of 14 μM of the proton carrier FCCP. An increased stationary current was observed according to a 20-fold higher specific conductance (35 nS/cm²).

To show that the light-induced signals after addition of PM suspension reflect the electrical activity of BR, narrow band interference filters were used to obtain the action spectrum of the signal. The result is shown in Fig. 4. The action spectrum is compared with the absorption spectrum of BR. Both curves are normalized to their maximal values.

Fig. 5 shows the relaxation time τ of the current density as a function of the reciprocal light intensity. At low

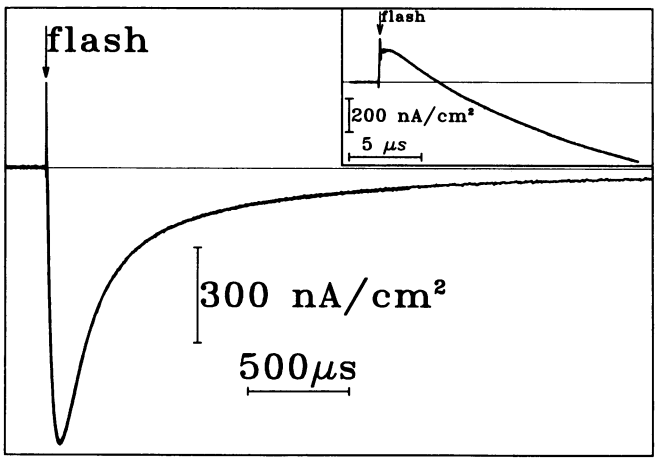

FIGURE 3 Bacteriorhodopsin. Dye-laser flash induced transient current density. The inset shows the beginning of the signal from the same experiment with higher time resolution. The rise of the BR signal is distorted by the photoartefact. The signals are averages from 128 single shots with a delay of Δt = 5 s between two shots. Conditions as in Fig. 2.

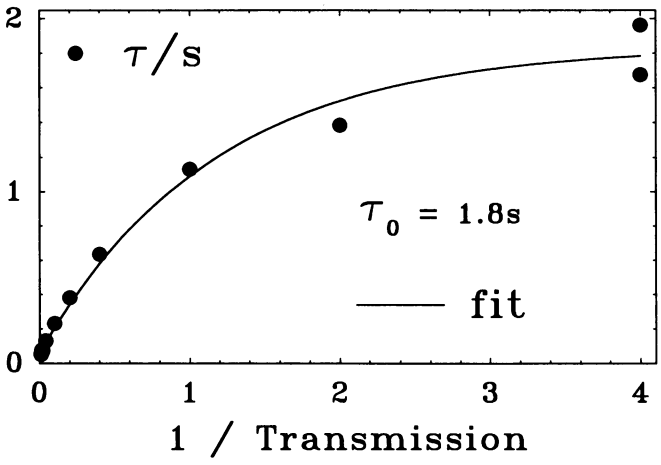

FIGURE 5 Bacteriorhodopsin. Reciprocal time τ^{-1} of relaxation of the initial current density of BR to its stationary value as a function of the light intensity (under stationary illumination). The solid line is a fit to the saturation function described in the text. τ_0 = 1.8 s is the extrapolation of the relaxation time τ for vanishing light intensity. Conditions as in Fig. 2.

intensities, the time constant saturates at $\tau_0 = (1.8 \pm 0.3)$ s.

To prove the correspondence between the electrical signal in the presence of PM fragments and the photocycle of bacteriorhodopsin fast kinetics of the electrical signal were studied. Fig. 3 shows a 570 nm dye-laser pulse induced electrical signal after addition of PM under the same conditions as in Fig. 2 except that the temperature was 19°C.

ATPases

Three different P-type ATPases were investigated: The Na,K-ATPase from pig kidney, the Ca-ATPase from sarcoplasmic reticulum from rabbit skeletal muscle, and the H,K-ATPase from pig gastric mucosa.

The Na,K-ATPase maintains the Na^+- and K^+-ion gradients in animal cells. In the presence of Mg^{2+}-ions for every hydrolyzed ATP-molecule three Na^+-ions are transferred outward and two K^+-ions are transported into the cell so that the enzyme transports one positive netcharge out of the cell. It has been shown previously that the electrical signal of the Na,K-ATPase on BLM corresponds to the Na^+-dependent steps of the reaction cycle (5, 12, 27). It can therefore also be observed in the absence of K^+.

The Ca-ATPase from sarcoplasmic reticulum is responsible for the relaxation of muscles. After muscle contraction for every hydrolyzed ATP molecule two Ca^{2+}-ions are removed from the cytoplasm to the lumen of the sarcoplasmic reticulum to lower the cytoplasmic Ca^{2+}-concentration.

The function of the H,K-ATPase from parietal cells of gastric mucosa is the acid secretion in the stomach and the maintenance of the low pH level of ~1 against a proton gradient of about 6 pH units. For every hydrolyzed ATP molecule, H^+-ions are secreted and K^+-ions are transfered into the parietal cells. The stoichiometry is 1:1 or 2:2. Therefore, under physiological conditions, the H,K-ATPase is electrosilent. However, under K^+-free conditions, the partial reaction of the electrogenic proton transport is observable (19).

To activate these ion pumps, a rapid concentration jump of ATP was produced by photolyzing caged ATP with an UV laser flash (11, 12). The obtained electrical signals with peak current densities of about 10 nA/cm^2 are shown in Fig. 6. In all three cases the obtained signals correspond to a translocation of positive charge towards the SSM.

Fig. 6, *A* and *B*, shows laser flash induced signals in the presence of Na,K-ATPase containing membrane fragments before and after inhibition with the specific inhibitor strophantidin (250 μM). After inhibition, only the artefact remained. The reason for the opposite direction of the artefact before and after inhibition is not known. Light induced signals in the presence of Ca- and H,K-ATPase containing vesicles are shown in Fig. 6, *C* and *D*, respectively. The H,K-ATPase could be inhibited with specific inhibitor SCH28080 (10 μM). In all three cases free ATP (1.6 mM) suppressed and vanadate (1 mM) inhibited the electrical signal and only an artefact remained similar to that one shown in Fig. 6 *B*.

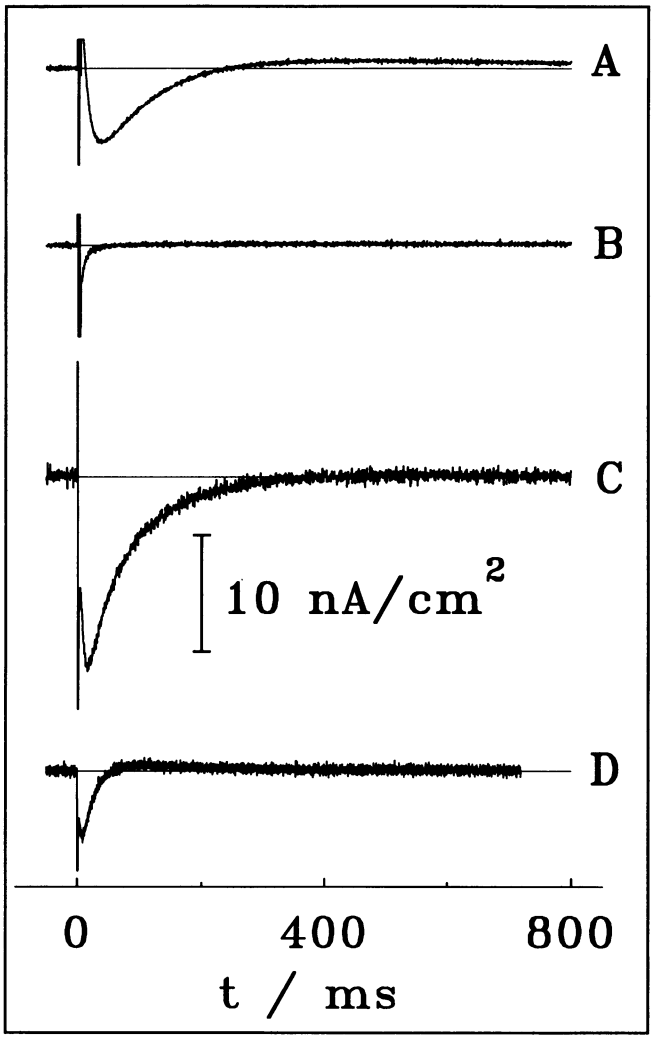

FIGURE 6 ATPases. (*A*) Light induced transient current density after addition of membrane fragments containing Na,K-ATPase from pig kidney. Conditions: SSM formed from PC + octadecyl amine; 130 mM NaCl, 3 mM $MgCl_2$, 25 mM imidazole/HCl, pH = 6.24, 100 μM caged ATP. (*B*) Conditions were the same as in *A* but 250 μM strophantidin were added. (*C*) Light induced transient current density after addition of vesicles containing Ca-ATPase from sarcoplasmic reticulum of rabbit skeletal muscle. Conditions: SSM formed from PC + octadecyl amine; 1 mM $CaCl_2$, 1 mM $MgCl_2$, 1 mM EGTA, 1 mM DTT, 20 mM MES/TRIS, pH = 6.23, 4 μM A23187, 280 μM caged ATP. (*D*) Light induced transient current density after addition of vesicles containing H,K-ATPase from pig stomach. Conditions: SSM formed from PC + PS; 50 mM imidazole, 3 mM $MgCl_2$, 1 mM DTT, 250 μM EGTA/TRIS, pH = 6.23, 260 μM caged ATP. Release rate of ATP from caged ATP in all cases: η = 4–8%.

DISCUSSION

BLMs have proven to be a versatile and sensitive tool for the investigation of the electrical properties of ion

pumps. Because of their low specific conductance and their high specific capacitance, they can be used as capacitive electrodes for the registration of pump currents generated by the protein containing membrane fragments or vesicles which are adsorbed to the BLM.

A variety of ion pumps was investigated with the SSM method. The currents generated by the proteins on a SSM were analyzed and compared with results obtained from analogue experiments on BLMs.

Lipid monolayers and bilayers on solid substrates have been produced in the past by a variety of techniques (26, 30, 31, 37, 38, 39, 43).

However, when supported by metal surfaces, some of these preparations had a relatively high conductance which made them unsuited for the investigation of the electrical properties of membrane proteins (e.g. (39, 43): $G > 100$ nS/cm^2).

Low conductance is required because only a part of the BLM or SSM surface is covered with adsorbed membrane fragments or vesicles. The uncovered surface acts as a shunt resistance which, if excessively low, leads to a high background noise current.

The electrical signals produced by ion translocating membrane proteins adsorbed to a SSM are similar to signals obtained with the BLM under comparable conditions. This gives evidence that the conductance of the SSM sample is sufficiently low to enable the use of the SSM in the same way as a conventional BLM as a capacitive electrode. In reference 13 it is shown that the specific conductance of a SSM fits to values measured for a BLM, although the conducting mechanism remains unexplained.

In addition to low specific conductance, high specific capacitance of the lipid membrane is required. The measured initial current I_0 is proportional to $C_m/(C_m + C_p)$ (4). Therefore, the specific capacitance C_m of the lipid membrane should be of the order of magnitude of the specific capacitance C_p of the protein containing adsorbed membrane fragment, to give large capacitive currents. The specific electrical capacitance C_p of a membrane fragment is ≈ 1 μF/cm^2. The value for the BLMs specific capacitance is ≈ 0.5 μF/cm^2.

Although the specific capacitance of the prepared SSMs is only one-fifth of the value measured for the bilayer, this value is sufficient to ensure large capacitive currents after activation of charge translocating membrane proteins.

An explanation for the lowered capacitance of the SSM might be that only a part of the lipid film on the solid support is sufficiently thin to give a substantial contribution to the capacitance. This interpretation is confirmed by the results presented by Florin and Gaub using surface plasmon microscopy (13).

A disadvantage of the SSM setup is its sensitivity to light. Especially at short wavelengths, radiation interacts with the gold surface and leads to a photoinduced electrical current. Control experiments to discriminate the protein generated signals from light induced artefacts are therefore crucial.

After addition of the PM suspension (Figs. 2 and 3), signals identical to those of PM adsorbed to BLM (8, 10, 18) are obtained. These signals differ from the photoartefact recorded before addition of PM. Under stationary illumination (Fig. 2) the signals are about three orders of magnitude larger than the artefacts.

The signal shown in Fig. 3 may be described by a sum of four exponentials. Using the fit procedure SPLMOD (29), we obtained the decay times $\tau_1 = 4.0$ μs, $\tau_2 = 52$ μs, $\tau_3 = 173$ μs, and $\tau_4 = 4.3$ ms. These values are comparable to the values obtained on BLM or gels (6, 9, 22, 40): $\tau_1 = 1.2$ μs, $\tau_2 = 50$ μs, $\tau_3 = 200$ μs, and $\tau_4 = 4$ ms. The difference found for the first component between the SSM and the BLM measurement is probably due to the superposition of rising BR-signal and the photoartefact in the case of the SSM method (see *inset* of Fig. 3).

The action spectrum of BR (Fig. 4) on a SSM agrees with the action spectrum on a BLM. This gives evidence that the light induced currents in the presence of a PM suspension are indeed due to the pump activity of BR.

According to the proposed microscopical structure of the SSM (Fig. 1 *C*) we suggest an equivalent circuit identical to that of a conventional BLM. The circuit is shown in Fig. 1 *D*. The time dependent pump current I_p of the membrane protein is distorted by the equivalent circuit described by the specific conductivities G_m, G_p, and the specific capacitances C_m, C_p of the SSM and the attached membrane fragments, respectively. An expression for the time dependent electrical current I measured in the outer circuit can be obtained by circuit analysis. The result (see reference 4) for stationary illumination after switching on a constant light source is

$$I(t) = I_\infty + (I_0 - I_\infty) \cdot e^{-t/\tau}. \tag{1}$$

Here I_0 is the initial current density, I_∞ is the stationary current density and τ is the decay time of the current density to its stationary value. This decay time depends on light intensity J according to:

$$\tau(J) = \frac{C_m + C_p}{G_m + G_p + I_{p,0}(J)/V^*}, \tag{2}$$

where the pump current $I_{p,0}$ is given by:

$$I_{p,0}(J) = I^s_{p,0} \cdot \frac{J}{J + J_{1/2}}, \tag{3}$$

and $J_{1/2}$ and V^* are constants.

Analysis of the intensity dependence of the relaxation time τ of the light induced current densities under stationary illumination yields the system time τ_0 which describes the discharging of the capacitance of the compound membrane (4). It is given as the zero intensity limit of Eq. 2:

$$\tau_0 = \frac{C_m + C_p}{G_m + G_p}. \quad (4)$$

For the BLM, $\tau_0 = 0.2$ s was found. In the case of PM adsorbed to SSM we obtained $\tau_0 = (1.8 \pm 0.3)$ s as indicated in Fig. 5. Taking into account that the SSM has a lower specific capacitance ($C_{m,SSM} \approx 1/5 \cdot C_{m,BLM}$) with respect to the BLM and at least comparable specific conductance ($G_{m,SSM} \approx G_{m,BLM}$) we conclude that the shunt conductivity $G_{p,SSM}$ must be smaller than that of the BLM. This may possibly be interpreted as a stronger adsorption of the fragments to the SSM.

To investigate ATP-driven ion pumps, concentration jump experiments were performed by releasing ATP from caged ATP. Fig. 6, *A*, *C*, and *D*, shows the light induced signals in the presence of caged ATP and Na,K-, Ca- and H,K-ATPase, respectively. The spikes close to $t = 0$ are photoartefacts. After decay of these artefacts for times larger than 5–10 ms, signals are observed dependent on the presence of both protein and caged ATP.

The signals could be inhibited by specific inhibitors and only the photoartefact as before protein addition remained. This gives strong evidence that the obtained signals represent pump currents of the investigated ATPases.

We characterized the time course of the pump currents using the program SPLMOD to fit a sum of three exponentials to the data (29). In the case of Na,K-ATPase from pig kidney the data shown in Fig. 6 *A* can be described by the following reciprocal time constants: $\tau_1^{-1} = 79\ s^{-1}$, $\tau_2^{-1} = 11\ s^{-1}$, and $\tau_3^{-1} = 1\ s^{-1}$. Under similar conditions 62 s^{-1}, 14 s^{-1}, and 3 s^{-1} were obtained for the BLM (12).

The first two time constants τ_1 and τ_2 have previously been assigned to the pump activity of the protein. In fact, measurements on SSM and BLM yield similar results for these constants. This holds also in the case of Ca- and H,K-ATPase containing vesicles.

For the signal from Na,K-ATPase measured on BLM τ_3 is interpreted as the time constant of the equivalent circuit given by its components G_m, C_m, G_p, and C_p via Eq. 4 and has a value of about 0.2 to 0.3 s. From the experiments with Na,K-ATPase containing membrane fragments on the SSM, we obtain $\tau_3 = 1$ s for the system time, i.e., as in the case of BR, the system time for the SSM is larger than the system time for the BLM. This again may be interpreted as a stronger adsorption of the membrane fragments to the SSM.

CONCLUSIONS

These results show that the electrical properties of the SSM and the BLM are comparable. The behavior of ion pumps contained in adsorbed membrane fragments or vesicles is similar as in the BLM system. We have therefore proposed a microscopical sandwich-like structure (Fig. 1 *C*, here in the case of an adsorbed membrane fragment containing Na,K-ATPase) combining models for the BLM and the mercaptan monolayer as proposed in (4, 5, 11, 12) and (1, 2, 3, 24, 42), respectively. As a consequence an equivalent circuit as shown in Fig. 1 *D* identical to that of the BLM setup (4, 5, 11, 12) is suggested.

It is demonstrated that the SSM can be used to investigate the electrical transport properties of membrane proteins in much the same way as shown for the BLM.

An important advantage of the SSM over the BLM is its mechanical stability leading to insensitivity to external vibrations and long lifetime. This is particularly important for experiments where rapid stirring or fast exchange of the electrolyte is desired.

Despite the strong similarities of the SSM and the BLM differences between these two methods remain unexplained. The conducting mechanism with the SSM is not yet understood. It is important to clarify which processes are responsible for the light artefacts, reduced specific capacitance and electrode potential and whether they can be reduced or avoided.

We like to thank E.-L. Florin and H. E. Gaub (Institut für Biophysik-E22, Technische Universität München, München/Garching, Germany) for technical support and intense and fruitful discussions.

We are indebted to D. Winau (Institut für Atom- und Festkörperphysik, Freie Universität Berlin, Berlin-Dahlem, Germany), M. Ruppel (Institut für Botanik, JWG Universität Frankfurt, Frankfurt/Main, Germany), K. Hartung, H.-J. Butt, and W. Stoeckenius (MPI für Biophysik, Frankfurt/Main, Germany) for support and discussion.

We thank E. Grell, W. Hasselbach, D. Oesterhelt, and M. Stengelin for provided chemicals and specimens.

This work was supported by Deutsche Forschungsgemeinschaft within SFB 169.

Received for publication 15 June and in final form 16 September 1992.

REFERENCES

1. Bain, C. D., and G. M. Whitesides. 1988. Molecular-level control over order in self-assembled monolayer films of thiols on gold. *Science (Wash. DC)*. 240:62–63.
2. Bain, C. D., E. B. Troughton, Y.-T. Tao, J. Evall, G. M. Whitesides, and R. Nuzzo. 1989. Formation of monolayer films by the spontaneous assembly of organic thiols from solution onto gold. *J. Am. Chem. Soc.* 111:321–335.
3. Bain, C. D., and G. M. Whitesides. 1989. Modeling organic surfaces with self-assembled monolayers. *Angew. Chem.* 101:522–528.
4. Bamberg, E., H.-J. Apell, N. A. Dencher, W. Sperling, H. Stieve, and P. Läuger. 1979. Photocurrents generated by bacteriorhodopsin on planar bilayer membranes. *Biophys. Struct. Mech.* 5:277–292.
5. Borlinghaus, R., H.-J. Apell, and P. Läuger. 1987. Fast charge translocations associated with partial reactions of the Na,K-pump. I. Current and voltage transients after photochemical release of ATP. *J. Membr. Biol.* 97:161–178.

6. Butt, H. J., K. Fendler, E. Bamberg, J. Tittor, and D. Oesterhelt. 1989. Aspartic acids 96 and 85 play a central role in the function of bacteriorhodopsin as a proton pump. *EMBO J.* 8:1657–1663.

7. McCray, J. A., L. Herbette, T. Kihara, and D. R. Trentham. 1980. A new approach to time-resolved studies of ATP-requiring biological systems: Laser flash photolysis of caged ATP. *Proc. Natl. Acad. Sci. USA.* 77:7237–7241.

8. Danzshazy, Z., and B. Karvaly. 1976. Incorporation of bacteriorhodopsin into a bilayer lipid membrane: a photoelectric-spectroscopic study. *FEBS Lett.* 72:136–138.

9. Drachev, L. A., A. D. Kaulen, V. P. Skulachev, and V. V. Zorina. 1987. The mechanism of H^+ transfer by bacteriorhodopsin. *FEBS Lett.* 226:139–144.

10. Fahr, A., P. Läuger, and E. Bamberg. 1981. Photocurrent kinetics of purple-membrane shetts bound to planar bilayer membranes. *J. Membr. Biol.* 60:51–62.

11. Fendler, K., E. Grell, M. Haubs, and E. Bamberg. 1985. Pump currents generated by the purified NaK+-ATPase from kidney on black lipid membranes. *EMBO J.* 4:3079–3085.

12. Fendler, K., E. Grell, and E. Bamberg. 1987. Kinetics of pump currents generated by the Na,K-ATPase. *FEBS Lett.* 224:83–88.

13. Florin, E.-L., and H.-E. Gaub. 1993. Painted supported lipid membranes. *Biophys. J.* 64:375–383.

14. Hartung, K., E. Grell, W. Hasselbach, and E. Bamberg. 1987. Electrical pump currents generated by the Ca^{2+}-ATPase of sarcoplasmic reticulum vesicles adsorbed on black lipid membranes. *Biochim. Biophys. Acta.* 900:209–220.

15. Hasselbach, W., and M. Makinose. 1963. Über den Mechanismus des Calcium-transports durch die Membranen des Sarkoplasmatischen Retikulums. *Biochem. Z.* 339:94–111.

16. Hasselbach, W. 1978. The reversibility of the sarcoplasmic calcium pump. *Biochim. Biophys. Acta.* 515:23–53.

17. Henderson, R. 1977. The purple membrane from halobacteriuzm halobium. *Annu. Rev. Biophys. Bioeng.* 6:67–109.

18. Herrmann, T. R., and G. W. Rayfield. 1978. The electrical response to light of bacteriorhodopsin in planar membranes. *Biophys. J.* 21:111–125.

19. van der Hijden, H. T. W. M., E. Grell, J. J. H. H. M. de Pont, and E. Bamberg. 1990. Demonstration of the electrogenicity of proton translocation during the phosphorylation step in gastric H^+K^+-ATPase. *J. Membr. Biol.* 114:245–256.

20. Jørgensen, P. L. 1974. Purification and characterization of ($Na^+ + K^+$)-ATPase. III. Purification from the outer medulla of mammalian kidney after selective removal of membrane components by sodium dodecylsulphate. *Biochim. Biophys. Acta.* 356:36–52.

21. Jørgensen, P. L. 1974. Purification and characterization of ($Na^+ + K^+$)-ATPase. IV. Estimation of the purity and of the molecular weight and polypeptide content per enzyme unit in preparations from the outer medulla of rabbit kidney. *Biochim. Biophys. Acta.* 356:53–67.

22. Keszthelyi, L., and P. Ormos. 1980. Electrical signals associated with the photocycle of bacteriorhodopsin. *FEBS Lett.* 109:189–193.

23. Läuger, P., R. Benz, G. Stark, E. Bamberg, P. C. Jordan, A. Fahr, and W. Brock. 1981. Relaxation studies of ion transport systems in lipid bilayer membranes. *Quart. Rev. Biophys.* 14:513–598.

24. Laibinis, P. E., J. J. Hichmann, M. S. Wrighton, and G. M. Whitesides. 1989. Orthogonal self-assembled monolayers: alkanethiols on gold and alkane carboxylic acids on alumina. *Science (Wash. DC).* 245:845–847.

25. Ljungström, M., L. Norberg, H. Olaisson, Chr. Wernstedt, F. V. Vega, G. Arvidson, and S. Mårdh. 1984. Characterization of proton-transporting membranes from resting pig gastric mucosa. *Biochim. Biophys. Acta.* 769:209–219.

26. Lukashev, K. P., S. Y. Zaitskev, A. A. Kononenko, and V. P. Zubov. 1989. Photo-electrical properties of bacteriorhodopsin in Langmuir films. *Stud. Biophys.* 132:111–118.

27. Nagel, G., K. Fendler, E. Grell, and E. Bamberg. 1987. Na^+ currents generated by the purified Na^+K^+-ATPase on planar lipid membranes. *Biochim. Biophys. Acta.* 901:239–249.

28. Oesterhelt, D., and W. Stoeckenius. 1974. Isolation of the cell membrane of *Halobacterium halobium* and its fractionation into re and purple membrane. *In* Methods in Enzymology. Biomembranes, Part A. S. Fleischer and L. Packer, editors. Academic Press. 667–678.

29. Provencher, S. W., and R. H. Vogel. 1983. Regularization techniques for inverse problems in molecular biology. *In* Progress in Scientific Computing. P. Deuflhard and E. Hairer, editors. Birkhäuser, Boston. 304–319.

30. Rothe, U., and H. Aurich. 1989. Lipid coated particles—A new approach to fix membrane-bound enzymes onto carrier surfaces. *Biotech. Appl. Biochem.* 11:18–30.

31. Rothe, U., H. Aurich, H. Engelhardt, and D. Oesterhelt. 1990. Oriented incorporation of bacteriorhodopsin into the lipid shell of phospholipid-coated polymer particles. *FEBS Lett.* 263:308–312.

32. Saccomani, G., H. B. Stewart, D. Shaw, M. Lewin, and G. Sachs. 1977. Characterization of gastric mucosal membranes. IX. Fractionation and purification of K^+-ATPase-containing vesicles by zonal centrifugation and free-flow electrophoresis technique. *Biochim. Biophys. Acta.* 465:311–330.

33. Scales, D., and G. Inesi. 1976. Assembly of ATPase protein in sarcoplasmic reticulum membranes. *Biophys. J.* 16:735–751.

34. Smith, T. 1980. The hydrophilic nature of a clean gold surface. *J. Coll. Interf. Sci.* 75:51–55.

35. Stoeckenius, W., and W. H. Kunau. 1968. Characterization of particulate fractions from lysed cell envelopes of *Halobacterium halobium* and isolation of gas vacuole membranes. *J. Cell. Biol.* 38:337–357.

36. Stoeckenius, W., R. H. Lozier, and R. A. Bogomolni. 1979. Bacteriorhodopsin and the purple membrane of halobacteria. *Biochim. Biophys. Acta.* 505:215–278.

37. Tamm, L. K. 1988. Lateral diffusion and fluorescence microscope studies on a monoclonal antibody specifically bound to supported phospholipid bilayers. *Biochemistry.* 27:1450–1457.

38. Thompson, N. L., A. A. Brian, and H. M. McConnell. 1984. Covalent linkage of a synthetic peptide to a fluorescent phospholipid and its incorporation into supported phospholipid monolayers. *Biochim. Biophys. Acta.* 772:10–19.

39. Tien, H. T., and Z. Salamon. 1989. Formation of self-assembled lipid bilayers on solid substrates. *Bioelectrochem. Bioenerg.* 22:211–218.

40. Trissl, H.-W. 1990. Photoelectric measurements of purple membranes. *Photochem. Photobiol.* 51:793–818.

41. von Tscharner, V., and H. M. McConnell. 1981. Physical properties of lipid monolayers on alkylated planar glass surfaces. *Biophys. J.* 36:421–427.

42. Ulman, A., J. E. Eilers, and N. Tillman. 1989. Packing and molecular orientation of alkanethiol monolayers on gold surfaces. *Langmuir.* 5:1147–1152.

43. Wardac, A., and H. T. Tien. 1990. Cyclic voltammetry studies of bilayer lipid membranes posited on platinum by self assembly. *Bioelectrochem. Bioenerg.* 24:1–11.